

Enlarged symmetry and coherence in arrays of quantum dots

A. V. Onufriev and J. B. Marston

Department of Physics, Brown University, Providence, Rhode Island 02912-1843

(Received 18 September 1998)

Enlarged symmetry characterized by the group $SU(4)$ can be realized in isolated semiconducting quantum dots. A Hubbard model then describes a pillar array of coupled dots, and at half-filling the system can be mapped onto an $SU(4)$ spin chain. The physics of these structures is rich as novel phases are attainable. The spins spontaneously dimerize, and this state is robust to perturbations that break $SU(4)$ symmetry. We propose ways to experimentally verify the existence of the dimerized phase. [S0163-1829(99)03419-0]

I. INTRODUCTION

Quantum dot arrays are a new arena for the study of strongly correlated electrons and the persistence of quantum coherence. Physical properties of a single semiconducting dot as well as tunneling between dots can be controlled over a wide range—a luxury not available to us in ordinary condensed materials. Recent advances in nanofabrication techniques offer the possibility of constructing artificial structures so small that the electronic level spacing is comparable to the charging energy. As a consequence, these structures can exhibit enlarged continuous symmetries not normally found in nature. In this paper we determine conditions under which a pillar of coupled semiconducting quantum dots realizes the group $SU(4)$ as a good symmetry and shows that the $SU(4)$ spins spontaneously dimerize—a phase of matter that would be difficult to attain with the smaller $SU(2)$ symmetry of electrons in generic quantum dots.

Continuous symmetries are ubiquitous in physics. Rotational invariance characterized by the group $O(3)$ permits the classification of atomic orbitals via integer angular momentum quantum numbers.¹ Spinning particles, such as electrons, are described by representations of the group $SU(2)$. Approximate $SU(3)$ isospin symmetry of hadrons has its origin in the light masses of the up, down, and strange flavors of quarks.² Unlike the case of electrons for which $SU(2)$ symmetry is exact, quarks can be described by $SU(3)$ only approximately since the masses of the quarks are not exactly equal. Nevertheless, the approximate $SU(3)$ symmetry is useful for classifying hadrons. We show how an approximate $SU(4)$ symmetry can be realized in quantum dot structures and we exploit its properties to describe novel phases that should emerge in these structures under certain conditions.

Consider a potential well with N degenerate eigenstates. Taking electron spin into account there are a total of $2 \times N$ degenerate states, and, if all of these states are equivalent, in a sense made precise below, we can think of them as realizing the fundamental representation of the $SU(2N)$ group. In other words, electrons placed in the shell can be considered as having $2N$ different, but equivalent, flavors instead of just the ordinary two flavors of spin up and spin down. It is important to note that $SU(2N)$ symmetry is *not* equivalent, in general, to the higher-spin representations of the usual $SU(2)$ group familiar from the quantum theory of angular

momentum. Rather, for $N > 1$, $SU(2N)$ is a different and larger symmetry.

Ordinary atomic orbitals might seem like a good candidate but, for real atoms, the enlarged symmetry is broken down to the usual $SU(2)$ symmetry by electron-electron interactions that lift the degeneracy. However, as Stafford and Das Sarma noticed,³ semiconducting quantum dots offer the possibility of realizing enlarged symmetries. Quantum dots can be thought of as artificial atoms^{4,5} with tunable parameters. To be precise, the electron mass is replaced by the smaller band mass $m_e \rightarrow m_b$, and the Bohr radius $a_B = \hbar^2 / (m_e e^2)$ is replaced by $a_B^* = \epsilon (m_e / m_b) a_B$. In GaAs, $m_b \approx 0.067 m_e$, the dielectric constant $\epsilon \approx 13$, and $a_B^* \approx 100 \text{ \AA}$, which is two orders of magnitude larger than its fundamental value. Electrons in a quantum dot are confined in a nonsingular potential often described⁶ as a short square well in the z direction and a simple parabola in the x - y plane, $V(x, y) = \frac{1}{2} m_b \omega_0^2 (x^2 + y^2)$, though our results do not depend on the detailed form of the potential as long as it has cylindrical symmetry. For the lowest mode in the z direction, the resulting harmonic-oscillator eigenenergies are $E_{n, l_z} = \hbar \omega_0 (2n + |l_z| + 1)$ where n and l_z are, respectively, the radial and angular momentum quantum numbers.

II. CONSTRUCTING AND COUPLING $SU(2N)$ QUANTUM DOTS

We propose a one-dimensional array of rotationally symmetric III-V semiconducting quantum dots arranged in a pillar⁷ and show how approximate $SU(4)$ symmetry can be realized in the structure. Given sufficient control over dot diameters and gate positions and biases,⁵ the lowest s level ($n = l_z = 0$) of each dot can be completely filled (with two electrons), and the next higher, fourfold degenerate p level with $n = 0$ and $l_z = \pm 1$, can be half-filled with two valence electrons,⁸ as shown in Fig. 1. Apart from configuration splitting (discussed below), the two p electrons realize a self-conjugate (particle-hole symmetric) representation of $SU(4)$. The dimension of this representation is six, which corresponds to the six distinct ways the two electrons can be placed in the four available p states.⁹ Once electron tunneling between the dots is turned on, there are four energy scales in the problem: the gross level spacing $\Delta E = \hbar \omega_0$ in each well, the on-site Coulomb repulsion energy U , which

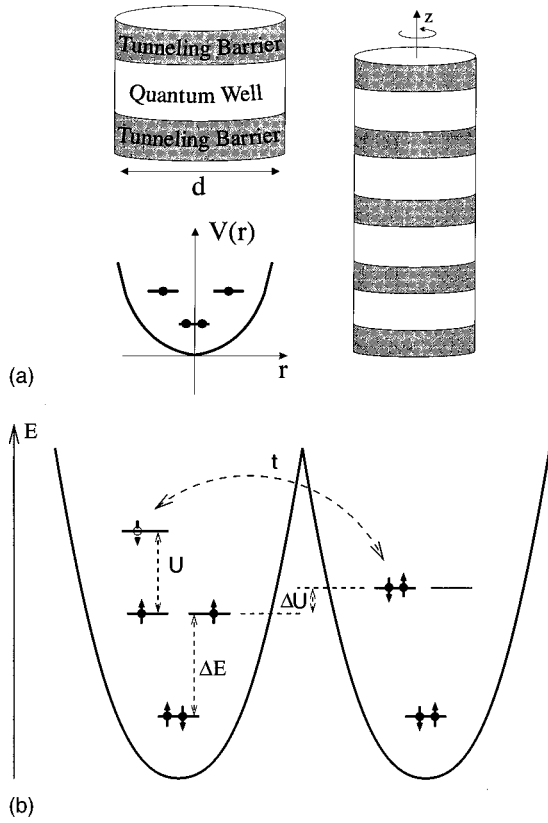


FIG. 1. (a) Individual quantum dot and proposed pillar array of quantum dots with approximate $SU(4)$ symmetry. By adjusting the bias, the lowest s level in each dot is filled completely and the first p level is half-filled with two electrons. (b) Energy diagram of two adjacent dots from the array. ΔU is the energy difference between the highest state of total orbital angular momentum $|L_z|=2$ (shown in the right dot) and the lowest state with $L_z=0$ (depicted in the left dot). An electron in a p level can temporarily hop into an empty level on an adjacent dot and then hop back. This virtual exchange process lowers its energy by the order of $J=4t^2/U$. If $U \gg \Delta U$ and $J \gg \Delta U$, all six configurations on each dot participate equally in the exchange, and the array realizes approximate $SU(4)$ symmetry.

represents the energy cost to add an additional electron to the dot, the energy splitting between the six different p -level configurations ΔU , and the tight-binding electron hopping amplitude $t > 0$ between states in adjacent wells, see Fig. 1(b).

The advantage of the proposed pillar array in Fig. 1(a) is clear: Conservation of the electron's orbital angular momentum around the z axis, a consequence of the cylindrical symmetry of the confining potential, guarantees that transitions between different angular momentum states in adjacent dots, which would break the flavor symmetry, are forbidden. The crucial conditions are that the energy gain J due to electron exchange between the dots greatly exceed ΔU , and also that the four flavors of electrons participate in the exchange on an equal footing. To second order in perturbation theory¹⁰ $J = 4t^2/U$ and thus we require

$$\frac{4t^2}{U} \gg \Delta U \quad \text{and} \quad U \gg \Delta U. \quad (1)$$

Another inequality ensures that only the p electrons play an active role in the low-energy physics:

$$\Delta E \gg t. \quad (2)$$

To estimate the size of ΔU for the p states in a quantum dot, we first note that spin-orbit coupling is negligible.¹¹ Thus ΔU is due almost entirely to the dependence of the electron-electron Coulomb interaction on the shell configuration as described by Hund's rules,¹² which have been shown both experimentally⁸ and theoretically^{13,14} to be directly applicable to semiconducting dots. The six configurations break up as: $6 \rightarrow 3 \oplus 1 \oplus 2$. The triply degenerate state of total orbital angular momentum $L_z=0$ and total spin $S=1$ is lowest in energy, the intermediate nondegenerate state has $L_z=0$ and $S=0$, and the twofold degenerate highest level has $|L_z|=2$ and $S=0$. As both ΔU and U scale as d^{-1} with dot size d , we may introduce $\Gamma \equiv \Delta U/U$, where Γ depends only on the shape of the dot and the confining potential. Lowest-order direct and exchange interaction integrals allow us to estimate that Γ ranges from 0.5 for thin, quasi-two-dimensional dots to $\Gamma=0.2$ for thick dots. Because the Coulomb interaction is long ranged, these numbers are nearly independent of the confining potential; indeed, $\Gamma \approx 0.2$ also holds for real (nearly spherical) atoms. For an electron in a potential well of characteristic size d we have: $\Delta E \approx \hbar^2/(m_b d^2)$, $U \approx e^2/(\epsilon d)$, and thus $\Delta E/U \approx a_B^*/d$. Symmetry-breaking effects due to the electron-electron interaction are therefore minimal in sufficiently small dots. To satisfy Eqs. (1) and (2) with $\Gamma=0.2$, simple algebra shows that we require $(\Delta E/U)^2 \gg 1$, which is in fact satisfied by small dots. For example, InAs/GaAs ($a_B^* \approx 300 \text{ \AA}$) quantum dots have been made¹⁵ that have $d \approx 200 \text{ \AA}$, $U \approx 18 \text{ meV}$, $\Delta E \approx 50 \text{ meV}$, and $(\Delta E/U)^2 \approx 8$. Adjusting the array spacing and the thickness of the insulating barriers, the hopping amplitude may be increased¹⁶ to $t = 0.2 \Delta E$. It then follows that $J \approx 20 \text{ meV}$. For dots that are not too thin, $\Gamma=0.2$, $\Delta U \approx 4 \text{ meV}$, and the crucial inequalities [Eqs. (1)] are satisfied. In contrast to these artificial atoms, there are no real atoms for which both inequalities [Eqs. (1) and (2)] hold because $\Delta E \approx U$ and $t \ll U$. A typical example is a copper oxide antiferromagnet¹⁷ with $J \approx 0.13 \text{ eV}$, $U \approx 10.5 \text{ eV}$, and hence $\Delta U \gg J$.

III. ARRAYS OF $SU(4)$ QUANTUM DOTS

Provided that the conditions outlined above are met, the pillar array of quantum dots may be described by an $SU(4)$ -invariant Hubbard model. We retain only nearest-neighbor hopping and on-site Coulomb repulsion and assume that no spin-flip or orbital-flip processes occur. Interdot Coulomb repulsion is not expected to change our results qualitatively. We use one Greek index $\alpha = 1, \dots, 4$ to label all four flavors of p states:³ $|l_z=1, s_z=+1/2\rangle \rightarrow |\alpha=1\rangle$, $|1, \downarrow\rangle \rightarrow |2\rangle$, $|-1, \uparrow\rangle \rightarrow |3\rangle$, and $|-1, \downarrow\rangle \rightarrow |4\rangle$. At half-filling the Hubbard Hamiltonian, for an open chain of length L sites, may be written

$$H = \sum_{i=1}^{L-1} t (c_i^\dagger c_{i+1} + \text{H.c.}) + \sum_{i=1}^L U [n(i) - 2]^2; \quad (3)$$

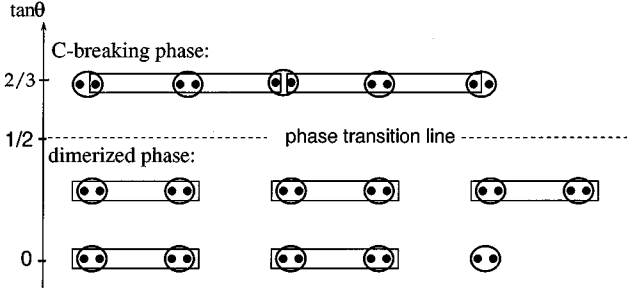


FIG. 2. Antiferromagnetic part of the SU(4) phase diagram for the isotropic, nearest-neighbor SU(4) spin chain. The two valence p electrons on each quantum dot are depicted by solid circles. SU(4) singlet bonds encapsulate four electrons and are depicted as rectangles. Chains with an odd number of artificial atoms have free spins at the chain ends in both the dimerized and the charge-conjugation (C -breaking) phases. For an even number of atoms, however, the dimerized phase has no free spins.

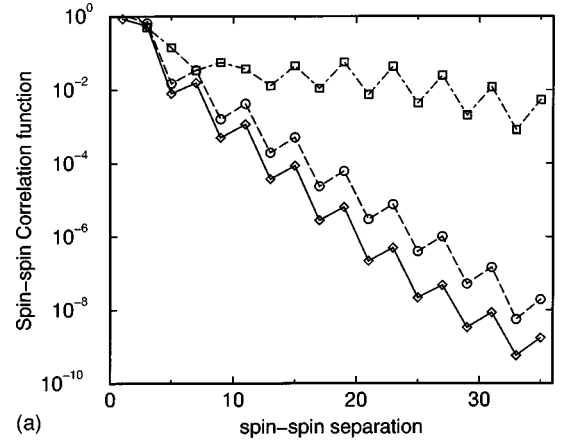
here repeated raised and lowered Greek indices are summed over, index i labels the dots, $c_i^{\dagger\alpha}$ is the creation operator for an electron in state α , and $n(i) \equiv c_i^{\dagger\alpha} c_{i,\alpha}$ is the total electron number operator at site i . Both the hopping and interaction terms in the Hamiltonian [Eq. (3)] are explicitly SU(4) invariant as can be easily checked by applying a unitary transformation, $c_i^{\dagger\alpha} \rightarrow U_{\beta}^{\alpha} c_i^{\dagger\beta}$, with $U^{\dagger}U = 1$, which leaves Eq. (3) unchanged.

At half-filling, the low-energy physics of the system is governed by the SU(4) spin degrees of freedom as creation of a charge excitation is energetically unfavorable. A weak-coupling renormalization-group (RG) calculation shows that umklapp scattering processes [which in the SU(4) case carry both charge and spin] drive the Hubbard model into a Mott-Hubbard insulating phase with gaps in both sectors.¹⁸ In the strong-coupling limit of $|t|/U \ll 1$, again there is a charge gap, and perturbation theory maps directly the Hubbard Hamiltonian [Eq. (3)] onto an insulating quantum antiferromagnetic Heisenberg spin chain. To $O(t^4/U^3)$, the effective Hamiltonian is

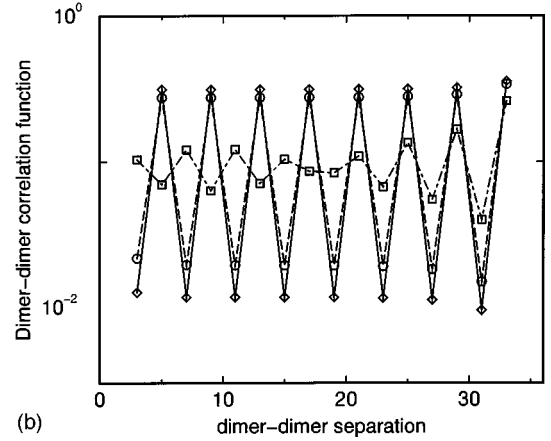
$$H_{\text{SU}(4)} = \frac{J}{2} \sum_{i=1}^{L-1} \left\{ \cos(\theta) \text{Tr}\{S(i)S(i+1)\} + \frac{1}{4} \sin(\theta) [\text{Tr}\{S(i)S(i+1)\}]^2 \right\} \quad (4)$$

plus next-nearest-neighbor terms. Here $S_{\beta}^{\alpha}(i) = c_i^{\dagger\alpha} c_{i\beta} - \frac{1}{2} \delta_{\beta}^{\alpha}$ are the 15 traceless SU(4) spin generators, the analogs of the three Pauli spin matrices in the familiar SU(2) case. With our summation convention $\text{Tr}\{S(i)S(j)\} \equiv S_{\beta}^{\alpha}(i) S_{\alpha}^{\beta}(j)$. The next-nearest-neighbor terms are $O(t^4/U^3)$ and $\tan(\theta) = C t^2/U^2$, where we find the constant $C > 0$; its exact value can be computed.¹⁹ The purely nearest-neighbor SU(4) spin chain was studied by Affleck, Arovas, Marston, and Rabson.²⁰ A combination of exact ground states, RG analysis, and conformal field theory permitted the determination of the entire phase diagram, the antiferromagnetic region of which is depicted in Fig. 2.

There is a spin gap at both weak and strong coupling; we therefore expect the gap to persist at all values of t/U . For



(a)



(b)

FIG. 3. DMRG calculation of (a) the spin-spin and (b) the dimer-dimer correlation functions for odd lattice separation and centered at the middle of a spin chain of length $L = 36$. Diamonds: $\theta = 0$; circles: $\theta = 0.2$; and squares: $\theta = 0.416$. The dimerized order diminishes as θ approaches $\theta^* = \tan^{-1}(1/2) \approx 0.4636$.

small values of t/U , θ is also small, and in the low-temperature limit ($T \ll J/k_b \approx 250$ K for the InAs/GaAs dot) the system is in a dimerized phase²¹ with broken translational symmetry, which can be qualitatively described as a set of nearest-neighbor SU(4) singlet bonds as depicted in Fig. 2. Spins not connected by a singlet bond are uncorrelated; in other words, each of the $6 \times 6 = 36$ possible configurations of spin and orbital momentum on two such sites are realized with equal probability. In contrast, spins on sites connected by a singlet bond are tightly constrained: there is zero amplitude for the same configuration to be found simultaneously on both of the sites. This has direct experimental consequences as explained below at the end of Sec. IV. The dimerized state, which also breaks reflection symmetry about site centers, has a large excitation gap since $O(J)$ energy is required to break a bond. Consequently spin-spin correlations decay exponentially as $\langle \text{Tr}\{S(i)S(j)\} \rangle \propto \exp(-|i-j|/\xi)$, where ξ is the spin-spin correlation length. White's infinite-size density-matrix renormalization-group²² (DMRG) analysis with open boundary conditions at the chain ends confirms this scenario²³ and determines ξ to be of order of the lattice spacing at $\theta = 0$, see Fig. 3(a). Another quantity of interest here is dimer-dimer correlation function, $\langle \text{Tr}\{S(i)S(i+1)\} \text{Tr}\{S(j)S(j+1)\} \rangle$, which tells us the probability to find a dimer on the link between sites i and $i+1$

given that there is one between sites j and $j+1$. The open boundary condition at the chain ends favors one of the two possible dimerization patterns, see Fig. 3(b). The amplitude of dimer-dimer correlation, the difference between its maximum and minimum values, can be used as an order parameter that provides a quantitative measure of the degree of dimerization.

It is interesting to note that dimer order can be achieved in ordinary translationally-invariant SU(2) antiferromagnetic chains only with large next-nearest-neighbor or biquadratic exchange. Here, however, the dimerized state at $\theta=0$ is a natural consequence of the enlarged SU(4) symmetry. For $\theta > \theta^* = \tan^{-1}(1/2) \approx 0.4636$, the chain is in a new phase of matter—not realizable for ordinary SU(2) chains—characterized by spontaneously broken charge-conjugation (C -breaking) symmetry, a spin gap, and extended singlet valence bonds.²⁰ The C -breaking state, unlike the dimerized state, breaks reflection symmetry about the centers of bonds, see Fig. 2. We find that the spin-spin correlation length increases, and the dimer-dimer order parameter decreases, as the system approaches the transition to the C -breaking phase at $\theta = \theta^*$, see Figs. 3(a) and 3(b). It may, however, be difficult to reach the C -breaking phase in experimental realizations of the system: as t/U is increased, terms in the effective Heisenberg model [Eq. (4)] such as the next-nearest-neighbor exchange $\text{Tr}\{S(i)S(i+2)\}$ become increasingly important. This term has a positive coefficient,¹⁹ favoring dimerized order.²⁴

IV. SYMMETRY BREAKING

It is important to establish whether or not the phases of the pure SU(4)-invariant system survive in the presence of symmetry-breaking processes. We show that the massive dimerized phase is robust in realistic experimental situations. The major symmetry-breaking process is due to electron-electron interactions that lift the sixfold degeneracy of the configurations of the two p electrons on each dot. The resulting ΔU in the Hubbard model induces SU(4)→SU(2) symmetry breaking both in the on-site energies ($6 \rightarrow 3 \oplus 1 \oplus 2$) and in the Heisenberg exchange term. Both perturbations can be incorporated by perturbing the SU(4)-invariant Hamiltonian [Eq. (4)] with two-body interaction terms of general bilinear form, which in the simplest case of a translationally invariant system can be written as

$$H'_{\text{Hund}} = \sum_{i=1}^L S_{\beta}^{\alpha}(i) T_{\alpha\nu}^{\beta\mu} S_{\mu}^{\nu}(i) + \sum_{i=1}^{L-1} S_{\beta}^{\alpha}(i) \tilde{T}_{\alpha\nu}^{\beta\mu} S_{\mu}^{\nu}(i+1). \quad (5)$$

SU(4) invariance is recovered by setting $T_{\alpha\nu}^{\beta\mu}, \tilde{T}_{\alpha\nu}^{\beta\mu} \propto \delta_{\nu}^{\beta} \delta_{\alpha}^{\mu}$; different choices for the tensors then realize all possible bilinear SU(4)→SU(2) symmetry-breaking terms. Other less important symmetry-breaking processes include (1) nonvanishing hopping between states in neighboring dots with different orbital angular momenta ($t_{\beta}^{\alpha} \neq t_{\beta}^{\alpha}$) also breaks SU(4)→SU(2), as again only spin symmetry remains. The breaking is minimized in the pillar array due to rotational symmetry about the vertical axis. (2) Spin-orbit coupling by itself breaks SU(4)→SU(2)⊗SU(2). However, this effect is small in semiconducting quantum dots.¹¹ (3) Nonmagnetic

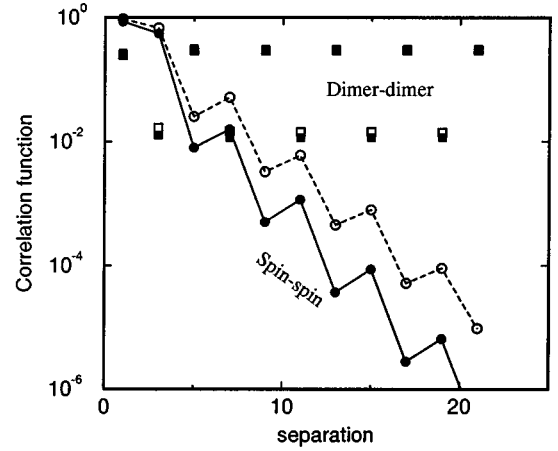


FIG. 4. DMRG calculation of the spin-spin (circles) and the dimer-dimer (squares) correlation functions for odd lattice separation and centered at the middle of the chain for the case $\theta=0$ and $L=36$. We compare the perfectly SU(4)-symmetric chain (solid symbols) to one with symmetry broken down to SU(2) via $\Delta U \neq 0$ (open symbols). For the broken symmetry case, the on-site tensor $T_{\alpha\nu}^{\beta\mu}$ has nonzero entries: $T_{12}^{21} = T_{21}^{12} = T_{34}^{43} = T_{43}^{34} = J/4$ and $T_{14}^{23} = T_{32}^{41} = T_{41}^{32} = T_{23}^{14} = T_{13}^{31} = T_{31}^{13} = T_{24}^{42} = T_{42}^{24} = J/4$. The nearest-neighbor tensor $\tilde{T}_{\alpha\nu}^{\beta\mu}$ has nonzero entries: $\tilde{T}_{33}^{33} = \tilde{T}_{34}^{34} = \tilde{T}_{43}^{43} = \tilde{T}_{44}^{44} = J/4$ and $\tilde{T}_{14}^{14} = \tilde{T}_{14}^{41} = \tilde{T}_{32}^{23} = \tilde{T}_{23}^{32} = J/8$.

impurities can lift the orbital degeneracy of a dot, breaking SU(4)→SU(2), as only spin symmetry remains intact. Spin-flip processes, induced by magnetic impurities or external magnetic fields, break SU(4) all the way down to discrete symmetries. It is essential to eliminate both magnetic and nonmagnetic impurities in and around the semiconducting dots.

The effects of SU(4)→SU(2) symmetry breaking may be analyzed numerically using the DMRG. We find that a block size of $M=36$ suffices for an accurate description of the massive phases. Even for large values of the symmetry-breaking parameter corresponding to $\Delta U \approx J$ the dimer long-range order persists, as is evident in Fig. 4.

Other symmetry-breaking mechanisms not included in the general bilinear Hamiltonian [Eq. (5)] can be incorporated by adding a one-body perturbation to the Hamiltonian [Eq. (4)],

$$H' = \lambda \sum_{i=1}^L S_{\beta}^{\alpha}(i). \quad (6)$$

In particular, spin-orbit coupling corresponds to

$$H'_{\text{SO}} = \lambda \sum_{i=1}^L [S_1^1(i) - S_2^2(i) - S_3^3(i) + S_4^4(i)]. \quad (7)$$

We have examined the effect of this coupling, Eq. (7), and have found that even for an unrealistically large value of $\lambda = J$ the dimerization pattern remains intact. The fact that the dimerized phase is robust is not surprising as the first excited state is separated by a large, of $O(J)$, energy gap from the ground state.

In the extreme limit $\Delta U \gg J$ of large SU(4) breaking according to Hund's rules, however, only the triply degenerate $S=1$ states survive and the chain is described by an ordinary spin-1 SU(2) quantum antiferromagnet, which is in a differ-

Haldane phase:

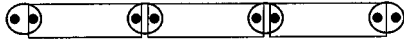


FIG. 5. The Haldane gap phase occurs when the $SU(4)$ symmetry is broken down to the usual $SU(2)$ spin symmetry of a spin-1 quantum antiferromagnet. $SU(2)$ singlet bonds, depicted as rectangles, involve just two electrons. Translational symmetry in the ground state is restored, and there are free spins at the chain ends both for odd and for even chain lengths.

ent massive phase, the Haldane gap phase,²⁵ with translational symmetry restored as shown in Fig. 5.

Transport measurements can be used to confirm the formation of a Mott-Hubbard charge gap at half-filling.^{26,27} To detect the dimerized spin structure experimentally, it may be possible to exploit the fact that, for an odd number of dots only, there are nearly free spins at the chain ends that will dominate the magnetic susceptibility. This feature distinguishes the dimerized state from other possible states of the $SU(4)$ spin chain such as the C -breaking and Haldane gap phases, which have free spins at chain ends for any number of sites (see Fig. 2). The free spins may be observable in sensitive electron spin resonance (ESR) measurements,²⁸ by scanning tunneling microscopy (STM) with a magnetized tip, or indirectly via optical spectroscopic experiments.²⁹

V. CONCLUSIONS

Isolated circular semiconducting dots, filled with a few electrons and free of impurities, have already been constructed and studied.⁸ We propose the construction of a pillar array of such circular dots. Approximate $SU(4)$ symmetry will be realized if some simple requirements are met. In particular, the dots must be small to minimize the symmetry-breaking effect of the intradot electron-electron interaction, which partially lifts the degeneracy of the six different electronic configurations. We predict that a chain of dots, at half-filling (four electrons per dot), will be in an insulating,

dimerized phase. Four to six dots will suffice because the correlation length is comparable to the lattice spacing, and the state should be robust to various types of symmetry-breaking processes as there is a nonzero spin gap to low-lying excitations. As a practical application of the proposed quantum dot array, there is the problem of quantum computation,³⁰ which requires a high degree of quantum coherence between computing elements. The dimerized phase is a strongly correlated state and could be used to test the degree of coherence in an array of quantum dots. In this it differs greatly from the standard Coulomb blockade seen in coupled dots, which operates independently of quantum coherence and, apart from the quantization of the electron charge, is classical. Indeed, quantum many-body phenomena such as the formation of long-range order are ideal tools to discern quantum coherence.

Finally we note two possible extensions of this work. Experimental evidence for the Kondo effect has been reported in transport measurements through a single quantum dot.³¹ It would be interesting to repeat the experiments with a $SU(4)$ dot as increasing the spin degeneracy enhances the Kondo effect.^{32,33} Also, the III-V dots discussed in this paper possess enlarged $SU(4)$ symmetry because the twofold orbital degeneracy combines with the usual twofold spin degeneracy. Alternatively, the natural valley degeneracy of silicon³⁴ could be exploited. In Si quantum wells, the twofold valley degeneracy is broken to twofold degeneracy by the Si/SiO₂ interface.³⁵ This remaining degeneracy, like the orbital degeneracy in the III-V dots, is enough to realize overall $SU(4)$ symmetry.

ACKNOWLEDGMENTS

The authors would like to thank Antal Jevicki, Jané Kondev, Sean Ling, and Alex Zaslavsky for fruitful discussions. The authors also thank Natalia Onufrieva for help with Fig. 1(a). Computational work was performed at the Theoretical Physics Computing Facility at Brown University. This work was supported in part by the National Science Foundation through Grants Nos. DMR-9313856 and DMR-9357613 and by a grant from the Alfred P. Sloan Foundation (J.B.M.).

¹Gordon Baym, *Lectures on Quantum Mechanics* (Benjamin/Cummings, Reading, MA, 1969), pp. 148–168.

²Claude Itzykson and Jean-Bernard Zuber, *Quantum Field Theory* (McGraw-Hill, New York, 1980), pp. 513–519.

³C. A. Stafford and S. Das Sarma, Phys. Rev. Lett. **72**, 3590 (1994).

⁴M. A. Kastner, Rev. Mod. Phys. **64**, 849 (1992); A. P. Alivisatos, Science **271**, 933 (1996).

⁵R. C. Ashoori, Nature (London) **379**, 413 (1996).

⁶B. Su, V. J. Goldman, and J. E. Cunningham, Phys. Rev. B **46**, 7644 (1992).

⁷J. J. Palacios and P. Hawrylak, Phys. Rev. B **51**, 1769 (1995).

⁸L. P. Kouwenhoven, T. H. Oosterkamp, M. W. S. Danoesastro, M. Eto, D. G. Austing, T. Honda, and S. Tarucha, Science **278**, 1788 (1997).

⁹The self-conjugate representation of $SU(4)$ differs from the fundamental representation considered recently by Y. Yamashita,

N. Shibata, and K. Ueda, Phys. Rev. B **58**, 9114 (1998). There is one electron in the fundamental representation, which therefore has dimension 4 and corresponds to quarter filling. At half-filling there are the two electrons, and the representation is self-conjugate.

¹⁰A more precise calculation of the exchange constant J is presented in G. Burkard, D. Loss, and D. P. DiVincenzo, Phys. Rev. B **59**, 2070 (1999).

¹¹Spin-orbit splitting of the p states is $O(10^3)$ to $O(10^5)$ times smaller than $\Delta E \equiv E_p - E_s$ because the splitting is of order $\hbar^2/(m_b^2 c^2) \langle r^{-1} dV(r)/dr \rangle = O(Z\alpha^2 \Delta E)$, where $\alpha \approx 1/137$ is the fine-structure constant and Z is the number of electrons in the dot [G. Baym, *Lectures on Quantum Mechanics* (Ref. 1), pp. 460–465].

¹²G. Baym, *Lectures on Quantum Mechanics* (Ref. 1), pp. 454–459.

¹³M. Koskinen and M. Manninen, Phys. Rev. Lett. **79**, 1389 (1997).

- ¹⁴O. Steffens, U. Rössler, and M. Suhrke, *Europhys. Lett.* **42**, 529 (1998); O. Steffens and U. Rössler, cond-mat/9711077 (unpublished).
- ¹⁵M. Fricke, H. Lorke, J. P. Kotthaus, G. Medeiros-Ribeiro, and P. M. Petroff, *Europhys. Lett.* **36**, 197 (1996).
- ¹⁶C. Livermore, C. H. Crouch, R. M. Westervelt, K. L. Campman, and A. C. Gossard, *Science* **274**, 1332 (1996).
- ¹⁷T. M. Rice, in *Strongly Interacting Fermions and High T_c Superconductivity*, Les Houches Lecture Series Session LVI (Elsevier Science, Amsterdam, 1995), pp. 19–67.
- ¹⁸J. B. Marston and I. Affleck, *Phys. Rev. B* **39**, 11 538 (1989).
- ¹⁹Perturbation in powers of t/U has been worked out for the SU(2) Hubbard model. See D. J. Klein and W. A. Seitz, *Phys. Rev. B* **8**, 2236 (1973); A. H. MacDonald, S. M. Girvin, and D. Yoshioka, *ibid.* **37**, 9753 (1988).
- ²⁰I. Affleck, D. Arovas, J. B. Marston, and D. Rabson, *Nucl. Phys. B* **366**, 467 (1991).
- ²¹I. Affleck, *J. Phys.: Condens. Matter* **2**, 405 (1990).
- ²²S. R. White, *Phys. Rev. Lett.* **69**, 2863 (1992); *Phys. Rev. B* **48**, 10 345 (1993).
- ²³The double-precision, vectorized, multiprocessor C code for the DMRG is run on a Cray EL-98 and J-916 computers [A. V. Onufriev and J. B. Marston (unpublished)].
- ²⁴The completely dimerized state is an exact ground state of $H_{\text{dimer}} = \sum_i [\text{Tr}\{S(i)S(i+1)\} + \frac{1}{2} \text{Tr}\{S(i)S(i+2)\}]$ as may be shown by rewriting H_{dimer} as a sum of projection operators.
- ²⁵F. D. M. Haldane, *Phys. Rev. Lett.* **50**, 1153 (1983); I. Affleck, T. Kennedy, E. H. Lieb, and H. Tasaki, *ibid.* **59**, 799 (1987).
- ²⁶C. Zhou, D. M. Newns, J. A. Misewich, and P. C. Pattnaik, *Appl. Phys. Lett.* **70**, 598 (1997); D. M. Newns, J. A. Misewich, C. C. Tsuei, A. Gupta, B. A. Scott, and A. Schrott, *ibid.* **73**, 780 (1998).
- ²⁷R. Kotlyar and S. Das Sarma, *Phys. Rev. B* **55**, 10 205 (1997); R. Kotlyar, C. A. Stafford, and S. Das Sarma, *ibid.* **58**, 1746 (1998).
- ²⁸M. Hagiwara, K. Katsumata, I. Affleck, B. I. Halperin, and J. P. Renard, *Phys. Rev. Lett.* **65**, 3181 (1990).
- ²⁹K. Leo, J. Shah, E. O. Gobel, T. C. Damen, S. Schmittrink, W. Schafer, and K. Kohler, *Phys. Rev. Lett.* **66**, 201 (1991).
- ³⁰See, for instance, D. P. DiVincenzo, *Science* **270**, 255 (1995); B. E. Kane, *Nature (London)* **393**, 133 (1998).
- ³¹D. Goldhaber-Gordon, H. Shtrikman, D. Mahalu, D. Abusch-Magder, U. Meirav, and M. A. Kastner, *Nature (London)* **391**, 156 (1998); S. M. Cronenwett, T. H. Oosterkamp, and L. P. Kouwenhoven, *Science* **281**, 540 (1998).
- ³²See, for example, A. C. Hewson, *The Kondo Problem to Heavy Fermions* (Cambridge University Press, New York, 1993).
- ³³J. Merino and J. B. Marston, *Phys. Rev. B* **58**, 6982 (1998).
- ³⁴See, for instance, Charles Kittel, *Introduction to Solid State Physics* (Wiley, New York, 1996).
- ³⁵S. J. Koester, K. Ismail, and J. O. Chu, *Semicond. Sci. Technol.* **12**, 384 (1997).